Zhu W Shiojima I (12 人略) Komuro I	IGFBP-4 is an inhibitor of canonical Wnt signalling required for cardiogenesis	Nature	454	345-349	2008
Monzen K Ito Y (9 人略) Komuro I	A crucial role of a high mobility group protein HMGA2 in cardiogenesis	Nat Cell Biol	10	567-574	2008
Yasuda N Miura S (16 人略) Komuro I	Conformational switch of angiotensin II type 1 receptor underlying mechanical stress-induced activation	EMBO Rep	9	179-186	2008
Sano M Minamino T (14 人略) Komuro I	p53-induced inhibition of Hif-1 causes cardiac dysfunction during pressure overload	Nature	446	444-448	2007
Tsutsumi T Ide T Tsutsui H (1 人略)	Modulation of the myocardial redox state by vagal nerve stimulation after experimental myocardial infarction	Cardiovasc Res	77	713-721	2008
Wu YW Naya M (5 人略) Tsutsui H (1 人略)	Heterogeneous reduction of myocardial oxidative metabolism in patients with ischemic and dilated cardiomyopathy using C-11 acetate PET	Circ J	72	786-792	2008
Makita N Behr E (13 人略) Tsutsui H (3 人略)	The E1784K mutation in SCN5A is associated with mixed clinical phenotype of type 3 long QT syndrome	J Clin Invest	118	2219-2229	2008
Naya M Tsukamoto T (5 人略) Tsutsui H	Olmesartan, but not amlodipine, improves endothelium-dependent coronary dilation in hypertensive patients	J Am Coll Cardiol	50	1144-1149	2007
Matsushima S Ide T (5 人略) Tsutsui H	Overexpression of mitochondrial peroxiredoxin-3 prevents left ventricular remodeling and failure after myocardial infarction in mice	Circulation	113	1779-1786	2006

Matsusaka H Ide T (5 人略) Tsutsui H	Targeted deletion of matrix metalloproteinase 2 ameliorates myocardial remodeling in mice with chronic pressure overload	Hypertension	47	711-717	2006
Matsusaka H Ide T (5 人略) Tsutsui H	Targeted deletion of p53 prevents cardiac rupture after myocardial infarction in mice	Cardiovasc Res	70	457-465	2006
Kitamura T Asai N (9 人略) Murohara T Takahashi M	Regulation of VEGF-mediated angiogenesis by the Akt/PKB substrate Girdin	Nat. Cell Biol	10	329-337	2008
Sugiura T Kondo T (7 人略) Murohara T	Nifedipine improves endothelial function : role of endothelial progenitor cell	Hypertension	52	491-498	2008
Li P Kondo T (4 人略) Murohara T	Role of bradykinin, nitric oxide and angiotensin II type 2 receptor in imidapril-induced angiogenesis	Hypertension	51	252-258	2008
Inoue N Kondo T (4 人略) Murohara T	Therapeutic angiogenesis using novel vascular endothelial growth factor-E/human placental growth factor chimera genes	Arterioscler Thromb Vasc Biol	27	99-105	2007
Cheng XW Kuzuya M (13 人略) Murohara T	Mechanisms underlying the impairment of ischemia -induced neovascularization in MMP-2-deficient mice	Circ Res	100	904-913	2007
Yokouchi K Numaguchi Y (6 人略) Murohara T	l-Caldesmon regulates proliferation and migration of vascular smooth muscle cells and inhibits neointimal formation after angioplasty	Arterioscler Thromb Vasc Biol	26	2231-223	2006
Numaguchi Y Sone T (7 人略) Murohara T	The impact of the capability of circulating progenitor cell to differentiate on myocardial salvage in patients with primary acute myocardial infarction	Circulation	114	I114-I119	2006

Ohara T Kim J Asakura M Asanuma H (5 人略) Kitakaze M	Plasma adiponectin is associated with plasma brain natriuretic peptide and cardiac function in healthy subjects	Hypertens Res	31	825-831	2008
Fujita M Asakura M (4 人略) Asanuma H (6 人略) Kitakaze M	Activation of ecto-5'-nucleotidase in the blood and hearts of patients with chronic heart failure	Journal of Cardiac Failure	14	426-430	2008
Liao Y Zhao H (2 人略) Asakura M Kim J Asanuma H Minamino T Takashima S Kitakaze M	Atorvastatin slows the progression of cardiac remodeling in mice with pressure overload and inhibits epidermal growth factor receptor activation	Hypertens Res	31	335-344	2008
Sanada S Asanuma H (6 人略) Kitakaze M (1 人略)	Long-term oral administration of dipyridamole improves both cardiac and physical status in patients with mild to moderate chronic heart failure : a prospective open-randomized study	Hypertens Res	30	913-919	2007
Asakura M Asanuma H Kim J (7 人略) Kitakaze M	Impact of adenosine receptor signaling and metabolism on pathophysiology in patients with chronic heart failure	Hypertens Res	30	781-787	2007
Kitakaze M Asakura M Kim J (1 人略) Asanuma H (3 人略) Minamino T (13 人略) J-WIND Investigators	Human atrial natriuretic peptide and nicorandil as adjuncts to reperfusion treatment for acute myocardial infarction(J-WIND):two randomised trials	Lancet	370	1483-1493	2007

Asanuma H (2 人略) Minamino T Takashima S (4 人略) Takahama H Kim J Asakura M (4 人略) Kitakaze M	S-nitrosylated and pegylated hemoglobin, a newly developed artificial oxygen carrier, exerts cardioprotection against ischemic hearts	J Mol Cell Cardiol	42	924-930	2007
Asanuma H Minamino T (1 人略) Kim J Asakura M Takashima S (1 人略) Kitakaze M	Blockade of histamine H2 receptors protects the heart against ischemia and reperfusion injury in dogs	J Mol Cell Cardiol	40	666-674	2006
Nakayama-Hamada M, Suzuki A Furukawa H Yamada R Yamamoto K	Citrullinated fibrinogen inhibits thrombin-catalysed fibrin polymerization	Journal of biochemistry	144	393-398	2008
Seguchi O Takashima S (1 人略) Asakura M (3 人略) Minamino T (1 人略) Furukawa H (9 人略) Kitakaze M	A cardiac myosin light chain kinase regulates sarcomere assembly in the vertebrate heart	J Clin Invest	117	2812-2824	2007

Journal of Molecular and Cellular Cardiology 46 (2009) 452–462

Contents lists available at ScienceDirect

Journal of Molecular and Cellular Cardiology

journal homepage: www.elsevier.com/locate/yjmcc

Original article

PKA rapidly enhances proteasome assembly and activity in in vivo canine hearts

Mitsutoshi Asai [a], Osamu Tsukamoto [a,b], Tetsuo Minamino [a,*], Hiroshi Asanuma [b], Masashi Fujita [a], Yoshihiro Asano [a], Hiroyuki Takahama [b], Hideyuki Sasaki [b], Shuichiro Higo [a], Masanori Asakura [b], Seiji Takashima [a], Masatsugu Hori [c], Masafumi Kitakaze [b]

[a] Department of Cardiovascular Medicine, Osaka University Graduate School of Medicine, Suita, 565-0871, Japan
[b] Department of Cardiovascular Medicine, National Cardiovascular Center, Suita 565-8565, Japan
[c] Osaka Medical Center for Cancer and Cardiovascular Diseases, Osaka 537-8511, Osaka, Japan

ARTICLE INFO

Article history:
Received 14 July 2008
Received in revised form 16 October 2008
Accepted 3 November 2008
Available online 13 November 2008

Keywords:
Proteasome
PKA
Phosphorylation
Assembly
Ubiquitinated protein
Ischemia/reperfusion

ABSTRACT

Proteasome regulates diverse cellular functions by eliminating ubiquitinated proteins. Protein kinase A (PKA) is a key regulator of proteasome activity. However, it remains unknown how PKA regulates proteasome activity and whether it controls proteasome activity in in vivo hearts. Both the in vitro peptidase assay and the in-gel peptidase assays showed that the treatment with PKA for 30 min dose-dependently activated purified 26S proteasome. Simultaneously, PKA treatment enhanced phosphorylation and assembly of purified 26S proteasome evaluated by non-reducing native polyacrylamide gel electrophoresis, either of which was blunted by the pretreatment with a PKA inhibitor, H-89. In in vivo canine hearts, proteasome assembly and activity were enhanced 30 min after the exogenous or endogenous stimulation of PKA by the intracoronary administration of isoproterenol or forskolin for 30 min or by ischemic preconditioning (IP) with 4 times of repeated 5 min of ischemia. The intracoronary administration of H-89 blunted the enhancement of proteasome assembly and activity by IP. Myocardial proteasome activity at the end of ischemia was decreased compared with the control, however, it did not differ from the control in dogs with IP. IP decreased the accumulation of ubiquitinated proteins in the canine ischemia/reperfusion myocardium, which was blunted by the intracoronary administration of a proteasome inhibitor, epoxomicin. However, proteasome activation by IP was not involved in its infarct size-limiting effects. These findings indicate that PKA rapidly enhances proteasome assembly and activity in in vivo hearts. Further investigation will be needed to clarify pathophysiological roles of PKA-mediated proteasome activation in ischemia/reperfusion hearts.

1. Introduction

The ubiquitin–proteasome system plays a major role in intracellular protein degradation and subsequently regulates cellular functions in various cells [1–4]. 26S proteasome is composed of 20S proteasome as its "core" catalytic unit capped on each end by 19S regulatory complex [5,6]. 26S proteasome is a cylinder-like structure containing 4 concentric rings, each containing 7 subunits. We have previously reported that impairment of proteasome activity may contribute to the progression of cardiac dysfunction along with the accumulation of ubiquitinated proteins in the pressure-overloaded heart of mice [7]. In addition, Bulteau et al. clearly demonstrated the deactivation of proteasome and the subsequent accumulation of ubiquitinated proteins in ischemia/reperfusion myocardium [8]. These findings suggest that impairment of the ubiquitin–proteasome system may be closely associated with cardiac diseases. Therefore, a better understanding the regulation of the ubiquitin–proteasome system may lead to new therapies for cardiac diseases. However, it remains largely unknown how proteasome is regulated in in vivo hearts.

There are several possible mechanisms that could regulate 26S proteasome activity, including 1) changes in protein levels of proteasome subunits, 2) post-translational modification of proteasome subunit such as phosphorylation/dephosphorylation, and 3) assembly/disassembly of proteasome subunits [9,10]. Recently, protein kinase A (PKA) is reported to be one of the key regulators of proteasome activity in the in vitro studies [11,12]. PKA increases proteolytic activities of the cardiac proteasome [11] and phosphorylation of the 19S proteasome subunit by PKA correlates with increased proteasome activity [12]. However, it remains to be resolved whether PKA increases proteasome activity by altering the status of proteasome assembly or by phosphorylating proteasome subunits. Thus, in the present study, we first investigated phosphorylation, assembly and activity of purified proteasome when it was treated with PKA. Next, we investigated proteasome assembly and activity in in vivo canine hearts when cardiac PKA was stimulated endogenously and

* Corresponding author. Tel.: +81 6 6879 3635; fax: +81 6 6879 3473.
E-mail address: minamino@medone.med.osaka-u.ac.jp (T. Minamino).

0022-2828/$ – see front matter © 2008 Elsevier Inc. All rights reserved.
doi:10.1016/j.yjmcc.2008.11.001

exogenously. We also checked the time-course changes in proteasome activity during ischemia/reperfusion period in dogs with and without endogenous PKA stimulation. Finally, we investigated the role of PKA-mediated proteasome activation by IP in the accumulation of ubiquitinated proteins and myocardial infarct size using a proteasome inhibitor.

2. Methods

2.1. Materials

Epoxomicin (a proteasome inhibitor), PKA, isoproterenol, forskolin and 2,3,5-triphenyltetrazolium chloride (TTC) were obtained from Sigma (St. Louis, MO, USA). A purified 26S proteasome from human erythrocyte and Suc-Leu-Leu-Val-Tyr-7-amino-4-methylcoumarin (proteasome peptidase substrates) were obtained from Biomol International (Plymouth Meeting, PA, USA). H-89 (a selective PKA inhibitor) and an antibody against serine/threonine phosphorylated proteins were obtained from Upstate (Lake Placid, NY, USA). Antibodies directed against ubiquitinated proteins (clone FK2) and proteasome subunits (Rpt5, α7, and β5) were purchased from Biomol International. Clone FK2 recognizes both mono- and poly-ubiquitinated proteins but not free ubiquitin, so the extent of protein ubiquitination could be determined.

2.2. Measurement of 26S proteasome activity

2.2.1. In vitro peptidase assay

The purified erythrocyte 26S proteasomes treated with various units of PKA with and without 100 μmol/L H-89

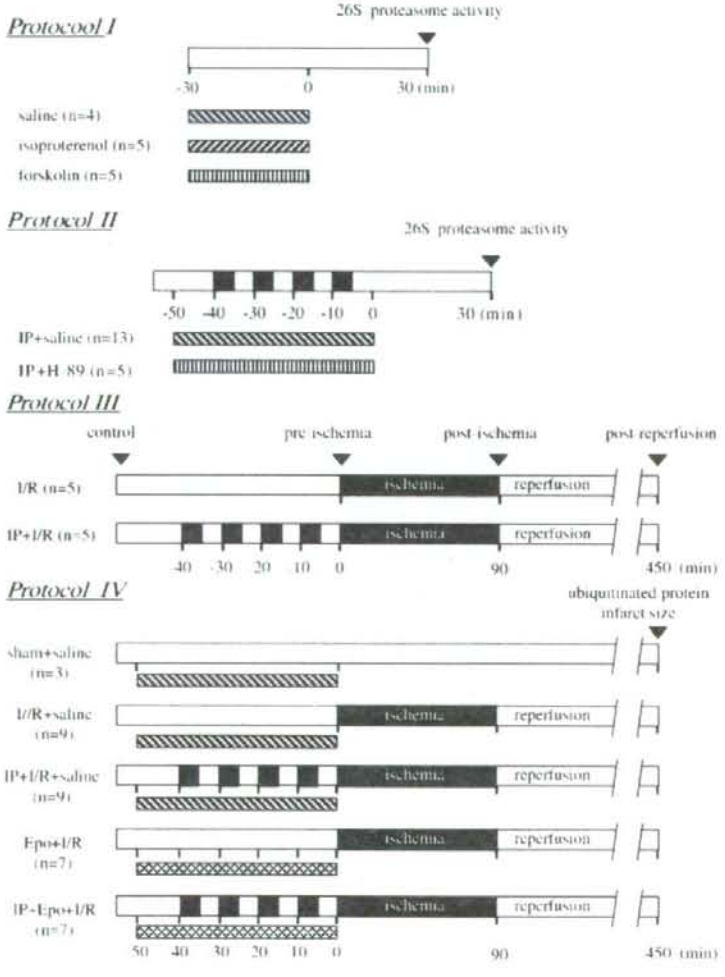

Fig. 1. Experimental protocols in canine model. (Protocol I) Effects of the intracoronary administration of saline ($n=4$), isoproterenol ($n=5$) or forskolin ($n=5$) (an exogenous stimulant of PKA) on proteasome activity in canine hearts. (Protocol II) Effects of ischemic preconditioning (IP) (an endogenous stimulant of PKA) with the intracoronary administration of saline ($n=8$ in LAD-perfused myocardium and $n=5$ in LCx-perfused one) or H-89 ($n=5$) (a PKA inhibitor) on proteasome activity in canine hearts. (Protocol III) Time-course changes in proteasome activity during ischemia/reperfusion period with and without IP ($n=5$ per each group). The triangle indicates the timing for myocardial biopsy. (Protocol IV) Effects of proteasome activation by IP on the accumulation of ubiquitinated proteins and infarct size in canine hearts. Sham operation was performed in 3 dogs. I/R and Epo indicate ischemia/reperfusion and epoxomicin, respectively.

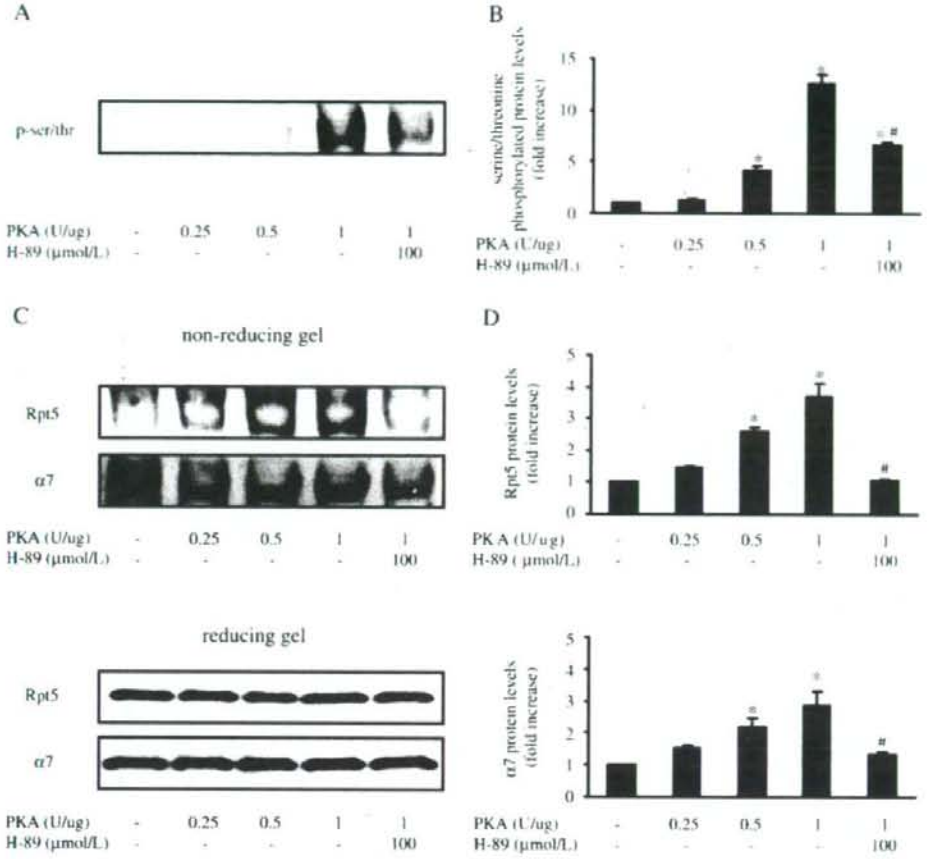

Fig. 2. PKA enhanced the activity of purified 26S proteasome. (A) Purified 26S proteasome activity detected by the in vitro proteasome peptidase assay. (B) Representative example of the 26S proteasome activity detected by in-gel peptidase assay using non-reducing gel electrophoresis. Purified 26S proteasome (1 μg) was applied to each lane. (C) Quantitative analysis of the 26S proteasome activity detected by in-gel peptidase assay. *$p<0.05$ vs. control. #$p<0.05$ vs. PKA (1 U/μg). $n=5$ per each group. Values are normalized to controls.

were incubated in assay buffer (50 mmol/L Tris–HCl, pH 7.5, 20 mmol/L $MgCl_2$, 1 mmol/L DTT, 50 μmol/L ATP) at 35 °C for 30 min. Then, they were incubated with proteasome activity assay buffer (50 mmol/L HEPES(pH 7.5), 5 mmol/L MgCl2, and 1 mmol/L DTT, 50 μmol/L ATP, 40 μmol/L LLVY-AMC) for 2 h at 37 °C. The fluorescence of each solution was measured by spectrophotometry .(HitachF-2000; Hitachi Instruments, Tokyo, Japan) with excitation at 390 nm (Ex) and emission at 460 nm (Em). All readings were standardized relative to the fluorescence intensity of an equal volume of free 7-amino-4-methylcoumarin (Sigma) solution (40 μmol/L).

2.2.2. In-gel peptidase assay

The purified 26S proteasome with different treatments were separated by non-reducing native PAGE using a modification of the method described previously [13]. We used a four gel layer consisting of equal amounts, from the bottom up, of 7.5, 5, 4, and 3% polyacrylamide. Non-reducing gels were run at 125 V for 2.5 h. The gels were incubated on a rocker for 1 h at 37 °C with 15 mL of 0.4 mmol/L Suc-LLVY-AMC in buffer (50 mmol/L Tris–HCl, pH 7.5, 5 mmol/L $MgCl_2$, 50 μmol/L ATP). Proteasome bands, whose density indicates 26S proteasome activity, were visualized on exposure to UV light and were photographed.

2.3. Evaluation of proteasome phosphorylation and assembly in vitro

MThe purified 26S proteasome with different treatments were separated by non-reducing native PAGE described above. Proteins on the non-reducing gels were transferred (110 mA) for 1.5 H onto polyvinylidene difluoride membranes. Western blotting analysis was carried out sequentially for detection of changes in phosphorylation state with anti phospho-serine/threonine antibody and for detection of 26S proteasome with anti Rpt5 or α7-subunit antibody. Antigens were visualized by a chemiluminescent horse-radish peroxidase method with the ECL reagent. A parallel reducing gel was used to confirm the total amount of 26S proteasome.

2.4. Animal instrumentation

Beagle dogs (Oriental Yeast, Osaka, Japan) weighing 8 to 12 kg were anesthetized with sodium pentobarbital (30 mg/kg, intravenously), and were prepared as previously described [14]. Briefly,

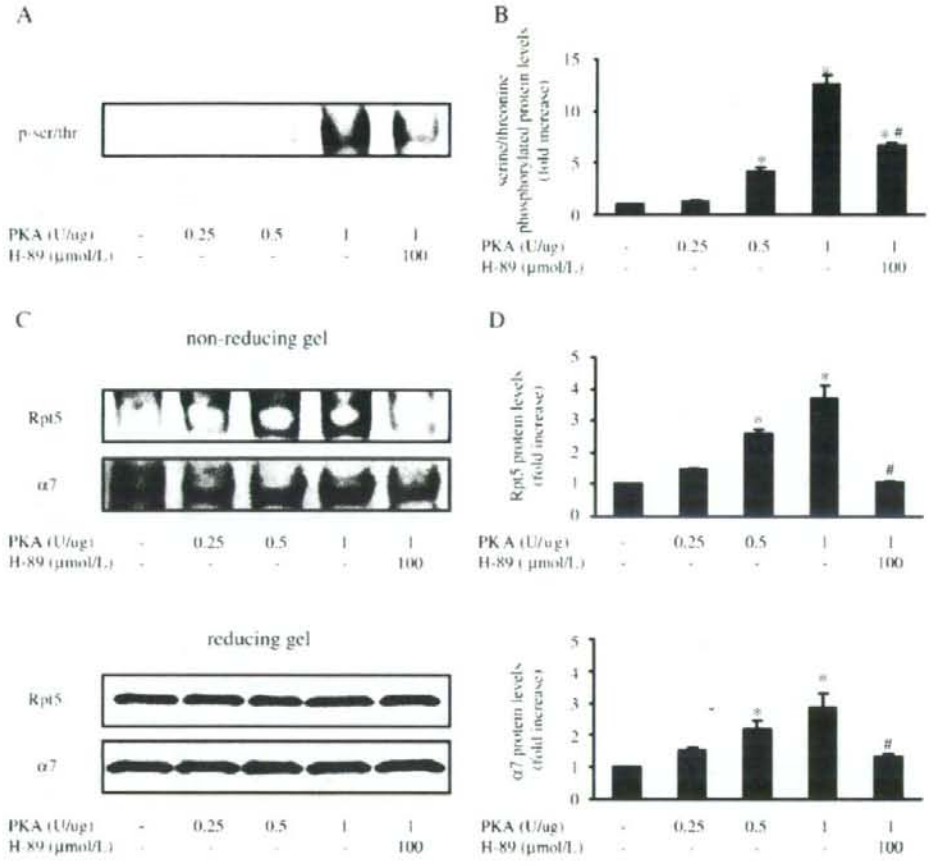

Fig. 3. PKA enhanced the phosphorylation and assembly of purified 26S proteasome. Representative example (A) and quantitative analysis (B) of 26S proteasome phosphorylation by Western blotting analysis with an anti phospho-ser/thr antibody. Representative example (C) and quantitative analysis (D) of Western blotting analysis on non-reducing gels. The status of 26S proteasome assembly was evaluated by Western blotting analysis with an anti-Rpt5 or anti-α7 antibody. Equal amounts of samples were loaded onto reducing and non-reducing gels. *$p<0.05$ vs. control, #$p<0.05$ vs. PKA (1 U/μg). $n=5$ per each group. Values are normalized to controls.

the trachea was intubated and each dog was ventilated by using room air mixed with oxygen. The chest was opened through the left fifth intercostal space, and the heart was suspended in a pericardial cradle. After heparinization (500 U/kg), the proximal portion of the left anterior descending coronary artery (LAD) was cannulated and perfused with blood via the carotid artery through an extracorporeal bypass tube. Both the coronary perfusion pressure (CPP) and heart rate (HR) were monitored during the experiments. In all experiments, CPP and HR were set at about 100 mmHg and 130 beats per min, respectively. This model was used to allow selective administration of agents to the LAD and reproduction of ischemia/reperfusion by clamping the bypass tube [15–17]. To examine the effects of PKA on proteasome activity in vivo, we employed isoproterenol or forskolin for exogenous stimulation of PKA and ischemic preconditioning (IP) for endogenous stimulation because PKA was reported to be activated by IP in canine hearts [15]. All procedures were performed in conformity with the Guide for the Care and Use of Laboratory Animals (NIH Publication No. 85-23, 1996 revision) and were approved by the Osaka University Committee for Laboratory Animal use.

2.5. Animal study protocols

2.5.1. Protocol I: Effects of isoproterenol or forskolin on proteasome activities in canine hearts

To assess the effects of exogenous PKA stimulation on proteasome activity, we selectively administrated saline ($n=4$), isoproterenol ($n=5$) or forskolin ($n=5$) into the LAD for 30 min in dogs. We preliminarily confirmed that the dose of ISO (10 μmol/L) used increased cAMP levels in the myocardium perfused by the LAD, but not in the myocardium of the left circumflex coronary artery (LCx) (data not shown). We determined the dose of forskolin (0.3 μg/kg/min) that activates PKA in canine hearts according to the previous report [18]. After administration, we rapidly sampled myocardial tissue from the LAD- and LCx-perfused myocardium as saline- or drug-treated myocardium and control one, respectively. Samples were placed into liquid nitrogen and stored at −80 °C (Fig. 1).

2.5.2. Protocol II: Effects of IP on proteasome activity in canine hearts

To assess the effect of endogenous PKA stimulation on the proteasome activity, we performed 4 cycles of 5 min coronary artery occlusion and a subsequent 5-minute period of reperfusion (IP) with

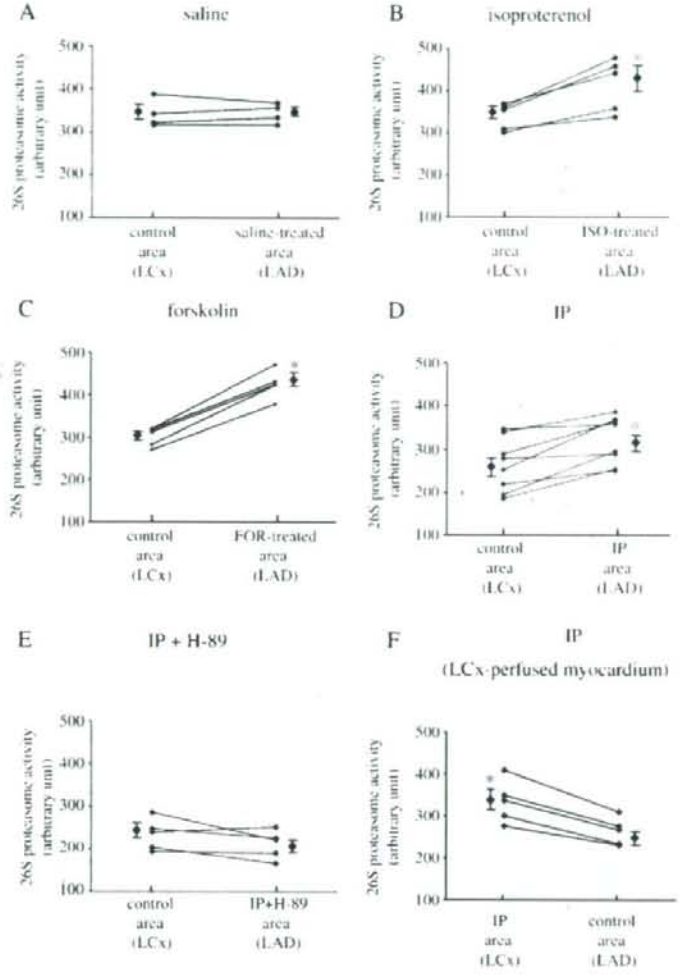

Fig. 4. Exogenous and endogenous PKA stimulation increased 26S proteasome activity in canine hearts. (A) 26S proteasome activity of canine hearts after sham operation in the control (LCx) or saline-treated (LAD) myocardium ($n=4$). (B, C) Effects of the exogenous PKA stimulation by the intracoronary administration of isoproterenol (ISO) or forskolin (FOR) on 26S proteasome activity in canine hearts ($n=5$). Effects of the endogenous PKA stimulation by ischemic preconditioning (IP) with saline (D) or H-89 (E) on 26S proteasome activity in canine hearts ($n=8$ and 5, respectively). (F) Effects of IP on 26S proteasome activity in the LCx-perfused myocardium ($n=5$) *$p<0.05$ vs. control area.

the intracoronary administration of saline ($n=8$) or H-89 (1.35 μg/kg per min) ($n=5$) for 50 min in dogs. The dose of H-89 was selected because the previous study showed this dose of H-89 inhibited the PKA activity in canine hearts [15,16]. At 30 min after IP, we rapidly sampled tissues from the LAD- and LCx-perfused myocardium, placed the samples into liquid nitrogen, and stored them at −80 °C. To confirm that proteasome activation by IP was not dependent on the myocardial area, we also performed the same IP protocol in LCx-perfused myocardium instead of LAD-perfused one in 5 dogs (Fig. 1).

2.5.3. Protocol III: Time-course changes in proteasome activity during ischemia/reperfusion period in canine hearts

To assess the time-course changes in proteasome activity during ischemia/reperfusion period in canine hearts, we underwent 90 min of ischemia followed by 6 h of reperfusion with and without IP in 10 dogs. Myocardial biopsy specimens were taken from LAD-perfused myocardium in each canine at 4 time-points: at the control, just before ischemia (pre-ischemia), at the end of 90 min ischemia (post-ischemia) and 6 h of reperfusion (post-reperfusion) (Fig. 1).

Fig. 5. PKA stimulation did not alter total protein levels of proteasome subunit in canine hearts. Representative example and quantitative analysis of Western blotting analysis of protein levels for 19S proteasome subunit Rpt5 as well as 20S proteasome subunits α7 and β5 in canine hearts after saline treatment (A), isoproterenol (ISO) treatment (B), forskolin (FOR) treatment (C), ischemic preconditioning (IP) (D), IP with H-89 (IP+H-89) (E). IP was performed in the LCx-perfused myocardium (F) instead of LAD-perfused one. CON and MW indicate control and molecular weight, respectively.

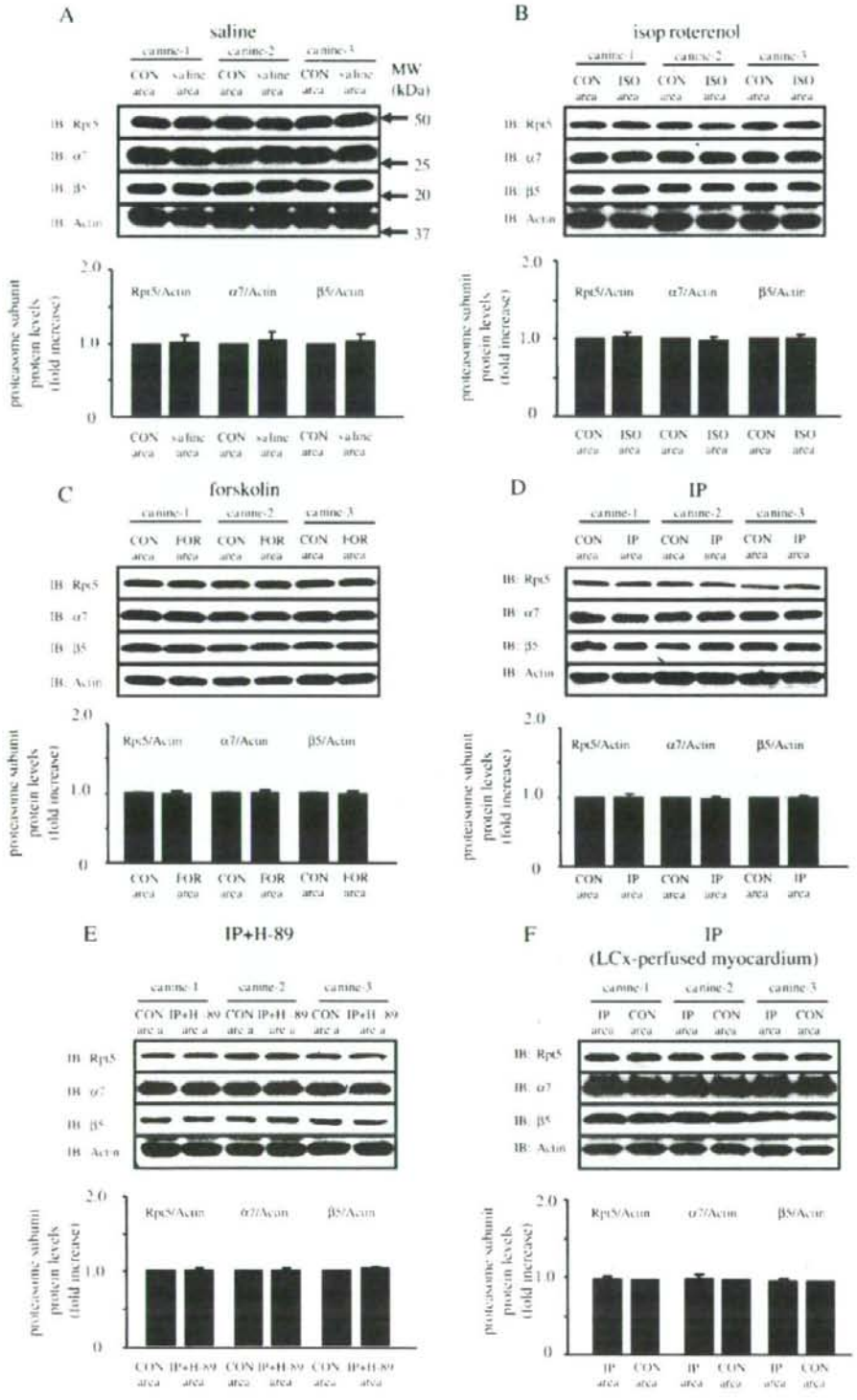
A
saline
B
isop roterenol
C
forskolin
D
IP
E
IP+H-89
F
IP
(LCx-perfused myocardium)
MW (kDa)
50
25
30
37
Rpt5/Actin
α7/Actin
β5/Actin
proteasome subunit protein levels (fold increase)
CON area
saline area
ISO area
FOR area
IP area
IP+H-89 area

2.5.4. Protocol IV: Effects of proteasome activation by IP on the accumulation of ubiquitinated proteins and infarct size in canine hearts

To assess pathophysiological roles of the proteasome in the ischemia/reperfusion myocardium, we intracoronarilly administered saline ($n=9$) or a proteasome inhibitor (epoxomicin at 2.5 μg/kg) ($n=7$) for 50 min and then we performed 90 min of ischemia followed by 6 h of reperfusion in dogs. To assess pathophysiological roles of the proteasome activation by IP in the ischemic/reperfused myocardium, we intracoronarilly administered a proteasome inhibitor (epoxomicin at 2.5 μg/kg) for 50 min with ($n=7$) and without IP ($n=9$) and then we performed 90 min of ischemia followed by 6 h of reperfusion in dogs. We preliminarily confirmed that this dose of epoxomicin reduced 26S proteasome activity by 43.0±6.2% ($n=3$) in the LAD-perfused myocardium compared with that in the LCx-perfused one. After 6 h of reperfusion, we rapidly sampled LAD-perfused myocardium, stored the samples at −80 °C, and investigated the level of the ubiquitinated proteins. We also evaluated the area at risk and the necrotic area after 6 h of reperfusion by Evans blue/TTC staining as described previously [19]. Myocardial infarct size was expressed as the necrotic area/area at risk (Fig. 1).

2.6. Purification of cardiac proteasome

Proteasome was purified from canine hearts according the method reported previously [20]. The peptidase assay was performed using the cytosolic fraction from the LAD- and LCx-perfused myocardium of canine hearts or the fractions containing 26S proteasomes separated on a 10–40% glycerol gradient centrifugation according to the method described above.

2.7. Western blotting analysis

Western blotting analysis was performed as described previously [21]. Immunoreactive bands were quantified by densitometry (Molecular Dynamics).

2.8. Statistical analysis

Data are expressed as the mean±SEM. Proteasome activities in LAD- and LCx-perfused myocardium were compared by the paired *t*-test. The time-course changes in proteasome activity during ischemia/reperfusion myocardium were analyzed by the two-way repeated analysis of variance (ANOVA) followed by Fisher's test. Other results were compared by the one-factor ANOVA followed by Fisher's test. In all analyses, $p<0.05$ was accepted as statistically significant.

3. Results

3.1. PKA enhanced the activity of purified 26S proteasome

The in vitro peptidase assay (Fig. 2A) and the in-gel peptidase assays (Figs. 2B, C) showed that the treatment of purified 26S proteasome with PKA enhanced 26S proteasome activity in a dose-dependent manner, while this effect was blocked by the pretreatment with H-89.

3.2. PKA enhanced the phosphorylation and assembly of purified 26S proteasome

Western blotting analysis of non-reducing gels probed with the antibody against serine/threonine phosphorylated proteins showed that PKA dose-dependently enhanced the phosphorylation of purified 26S proteasome (Figs. 3A, B). The phosphorylation of 26S proteasome was blocked by the pretreatment with H-89 (Figs. 3A, B). Interestingly, Western blotting analysis of non-reducing gels probed with the antibody against Rpt5 or α7 revealed that PKA dose-dependently increased either protein level that corresponded to 26S proteasome, which was blunted by H-89 (Figs. 3C, D upper panel). Western blotting analysis of reducing gels showed that the purified 26S proteasome were equally loaded to each lane (Figs. 3C, D lower panel). These results suggest that PKA enhanced the phosphorylation and assembly of proteasome, which may lead to the increase in proteasome activity.

3.3. PKA stimulation increased 26S proteasome activity in canine hearts

We found no differences in the proteasome activity in the saline-treated (LAD-perfused) and the control (LCx-perfused) myocardium (Fig. 4A). In contrast, exogenous and endogenous PKA stimulation by the selective intracoronary administration of isoproterenol or forskolin and IP, respectively, significantly increased 26S proteasome activity in LAD-perfused myocardium compared with that in LCx-perfused one (Figs. 4B, C, D). The selective intracoronary administration of a PKA inhibitor, H-89, blocked proteasome activation by IP (Fig. 4E). We confirmed that proteasome activation by IP in LCx-perfused myocardium was the same as that in LAD-perfused one (Fig. 4F). These results suggest that exogenous and endogenous PKA stimulation increased 26S proteasome activity in canine hearts.

3.4. PKA stimulation did not alter total protein levels of proteasome subunits in canine hearts

We found no differences in the total protein levels of proteasome subunits in the saline-treated (LAD-perfused) and the control (LCx-perfused) myocardium (Fig. 5A). Then, we examined the changes in protein levels of the proteasome subunits such as Rpt5, α7 and β5 in LAD- and LCx-perfused myocardium when proteasome was activated by exogenous and endogenous PKA stimulation in canine hearts. Importantly, there were no differences in the total protein levels of 3 proteasome subunits (Rpt5, α7, β5) in groups tested (Figs. 5B–F). These results suggest that exogenous and endogenous PKA stimulation did not alter total protein levels of proteasome subunits in the in vivo canine hearts.

3.5. PKA stimulation enhanced 26S proteasome activity and assembly in canine hearts

Since we found 26S proteasome activity of canine hearts mainly in the fractions 17–19 after glycerol gradient centrifugation (Figs. 6A–F, upper panels), samples from fractions 15–21 in the LCx- and LAD-perfused myocardium were immunoblotted with antibodies against Rpt5, α7 or β5 (Figs. 6A–F, lower panels). Consistently, Western blotting analysis with SDS-PAGE gel showed that proteasome subunit Rpt5, α7 or β5 was found mainly in fractions 17–19 (Figs. 6A–F, lower panels).

Fig. 6. Exogenous and endogenous PKA stimulation enhanced 26S proteasome assembly in canine hearts. Representative analysis of 26S proteasome activity (upper panel) and Western blotting analysis of proteasome subunits (lower panel) in the control and treated myocardium. The number indicated fractions separated on a 10–40% glycerol gradient centrifugation. (A) saline, (B) isoproterenol (ISO), (C) forskolin (FOR), (D) ischemic preconditioning (IP), (E) IP with H-89 (IP+H-89), (F) IP in LCx-perfused myocardium. (G) Quantitative analysis of 26S proteasome activity in canine hearts. Proteasome activity was expressed as the summation of proteasome activity in fractions 17–19 in the treatment myocardium which were divided by that in the same fractions in the control one ($n=4$ to 8 each). (H) Quantitative analysis of proteasome assembly in canine hearts. Proteasome assembly was expressed as the summation of Rpt5 protein levels in fractions 17–19 in the treatment myocardium which were divided by that in the same fractions in the control ones ($n=4$ to 8 each). *$p<0.05$ vs sham. #$p<0.05$ vs IP+H-89.

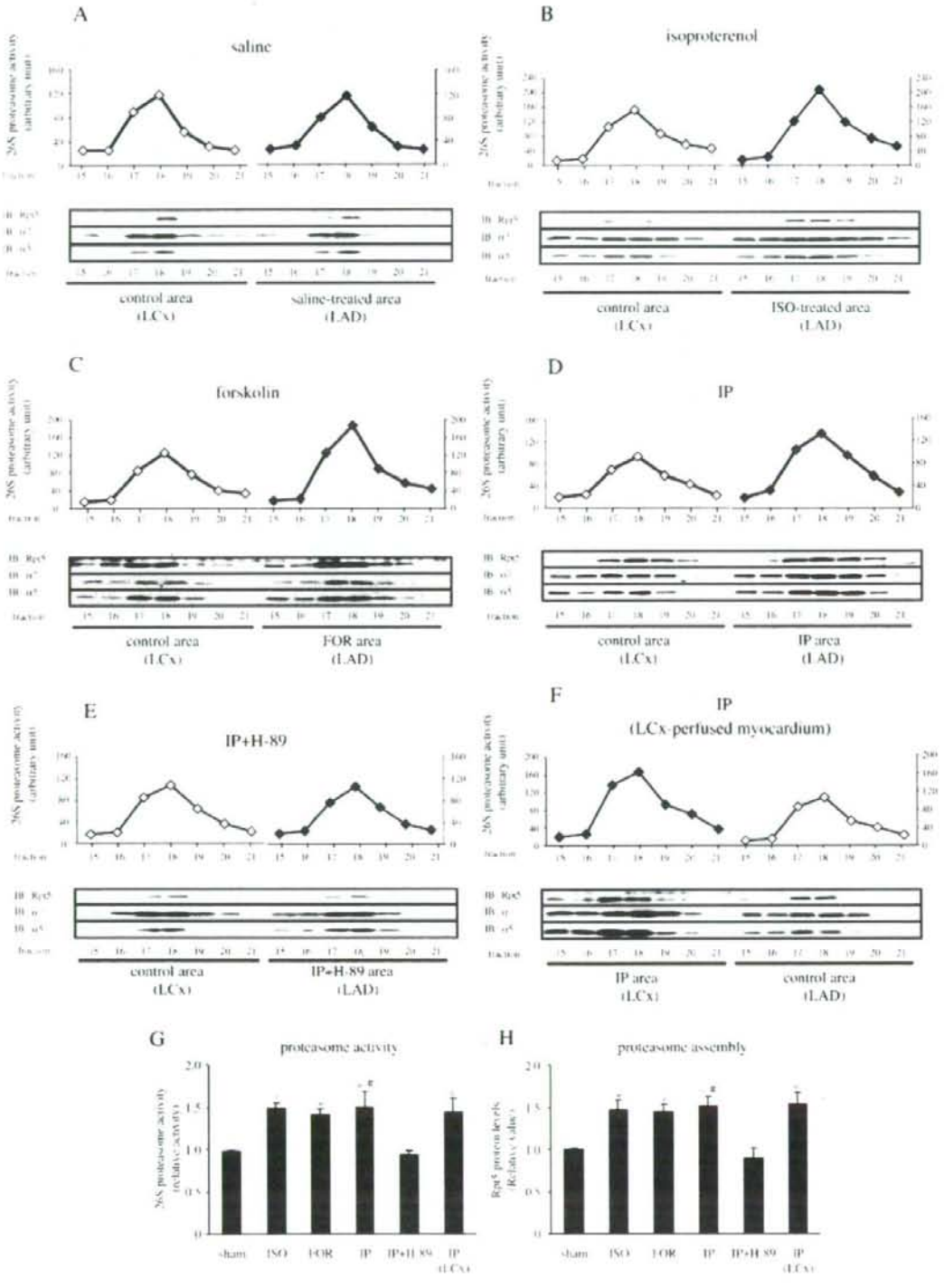
A
saline
control area
(LCx)
saline-treated area
(LAD)
B
isoproterenol
control area
(LCx)
ISO-treated area
(LAD)
C
forskolin
control area
(LCx)
FOR area
(LAD)
D
IP
control area
(LCx)
IP area
(LAD)
E
IP+H-89
control area
(LCx)
IP+H-89 area
(LAD)
F
IP
(LCx-perfused myocardium)
IP area
(LCx)
control area
(LAD)
G
proteasome activity
sham
ISO
FOR
IP
IP+H-89
IP
(LCx)
H
proteasome assembly
sham
ISO
FOR
IP
IP+H-89
IP
(LCx)

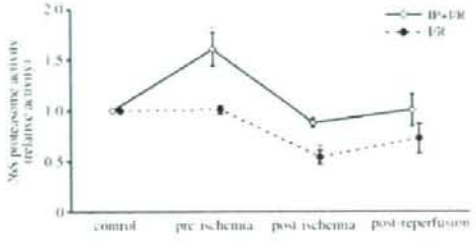

Fig. 7. Time-course changes in proteasome activity during ischemia/reperfusion period. Proteasome activity during ischemia/reperfusion period with and without IP. Myocardial biopsy specimens were taken at the control, just before ischemia (pre-ischemia), at the end of 90 min of ischemia (post-ischemia) and 6 h of reperfusion (post-reperfusion). Proteasome activity in IP+I/R and I/R groups was normalized to the corresponding control ones. IP+I/R and I/R indicate ischemia/reperfusion with and without IP, respectively. *$p<0.05$ vs control at the corresponding group.

Fig. 6 showed the representative proteasome activity and assembly using the myocardial sample of canine-1 in each groups in Fig. 5. Since we confirmed that the total amount of proteasome subunits were same in the control and treated myocardium, the alteration in protein levels of proteasome subunits in proteasome enriched fractions 17–19 indicate the alternation in the status of proteasome assembly. No differences were found in protein levels of proteasome subunits in the saline-treated (LAD-perfused) and the control (LCx-perfused) myocardium (Fig. 6A). Importantly, along with the increase in proteasome activity, the exogenous and endogenous PKA stimulation by isoproterenol, forskolin and IP significantly increased the protein levels of 3 different proteasome subunits in fractions 17–19 in the LAD-perfused myocardium compared with those in LCx-perfused one (Figs. 6B–D). Moreover, the selective administration of H-89 blunted the increases in protein levels of 3 different proteasome subunits and proteasome activation by IP in fractions 17–19 in the LAD-perfused myocardium (Fig. 6E). We also confirmed that the same findings were induced by IP in LCx-perfused myocardium (Fig. 6F). Quantitative analysis also showed that PKA enhanced proteasome activity and assembly, both of which were expressed as the summation of proteasome activity and Rpt5 protein levels in fractions 17–19 in the treatment myocardium which were divided by that in the same fractions in the control one, respectively (Figs. 6G, H). These results suggest that PKA stimulation enhanced 26S proteasome assembly and activity in canine hearts without alteration of total protein levels of proteasome subunits.

3.6. Time-course changes in proteasome activity during ischemia/reperfusion period with and without IP

The analysis of consecutive myocardial biopsy samples also revealed that IP increased the proteasome activity in the LAD-perfused myocardium in the same dog (Fig. 7). In canine hearts with IP, the proteasome activities at the post-ischemia and post-reperfusion were significantly lower than that at the pre-ischemia (≈just after IP), but they did not differ from the control. In canine hearts without IP, the proteasome activity at the post-ischemia was significantly decreased compared with that at the control or pre-ischemia (Fig. 7). Myocardial proteasome activity at the post-reperfusion did not differ from that at the post-ischemia in groups with and without IP (Fig. 7).

3.7. IP blunted the accumulation of ubiquitinated proteins in ischemia/reperfusion myocardium

To examine the pathophysiological role of proteasome activation by IP, we investigated effects of IP on the accumulation of ubiquitinated proteins, which may predict recovery of postischemic cardiac function [22], in the ischemia/reperfusion myocardium in canine model. Western blotting analysis revealed that ubiquitinated proteins were increased in ischemia/reperfusion myocardium, while their accumulation was attenuated by IP (Figs. 8A, B). The reduction in

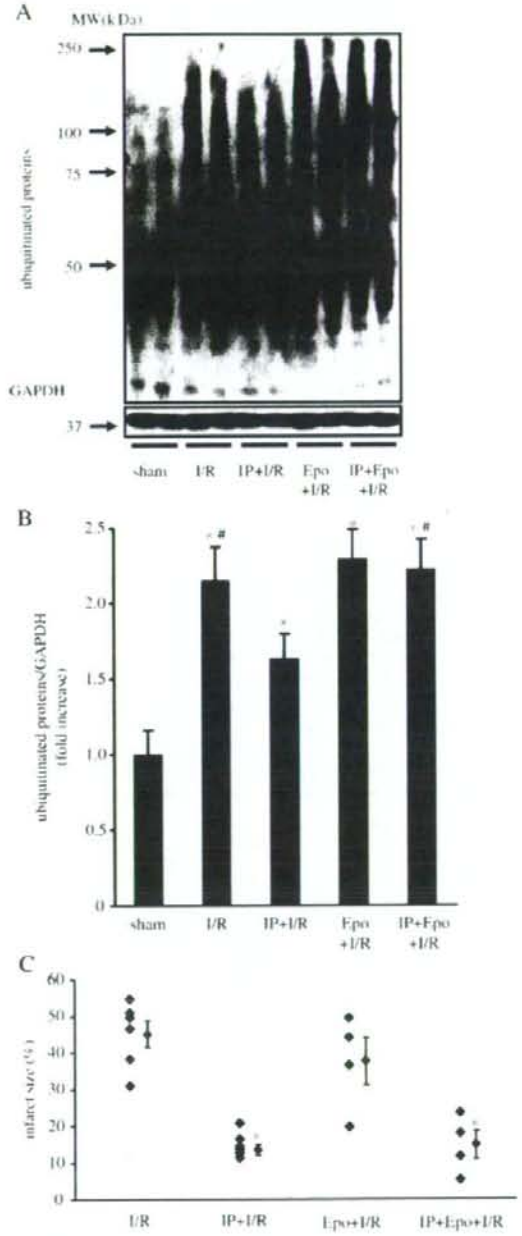

Fig. 8. Pathophysiological role of the enhancement of proteasome activity by IP. Representative example (A) and quantitative analysis (B) of Western blotting analysis of ubiquitinated proteins in canine ischemia/reperfusion (I/R) myocardium. *$p<0.05$ vs. sham, #$p<0.05$ vs. IP+I/R, $n=3$ per group. Values were normalized to sham. (C) Myocardial infarct size. *$p<0.05$ vs. I/R. MW, IP and Epo indicate molecular weight, ischemic preconditioning and epoxomicin (a proteasome inhibitor), respectively.

accumulated ubiquitinated proteins by IP was blunted by a proteasome inhibitor, epoxomicin. These results indicate that proteasome activation by IP alleviated the accumulation of ubiquitinated proteins in canine ischemia/reperfusion hearts.

3.8. Proteasome inhibition did not alter infarct size in canine hearts with and without IP

Fig. 8C showed the infarct size for each group in protocol IV. The intracoronary administration of epoxomicin before ischemia did not alter infarct size in this canine model. Consistent with the previous reports [15], we found that IP reduced myocardial infarct size. The infarct size-limiting effects of IP were not affected by the intracoronary administration of epoxomicin during IP procedure.

4. Discussion

4.1. PKA rapidly enhances phosphorylation, assembly and activity of 26S purified proteasome

Proteasome regulates cellular functions by eliminating ubiquitinated proteins [1–4]. Proteasome activity is enhanced by an increase in the levels of proteasome subunit proteins and their assembly, as well as by the post-translational modification of proteasome subunit through processes such as phosphorylation/dephosphorylation [9,10]. Recent studies have shown that PKA can phosphorylate several sites and increase proteasome activity in vitro [11,12]. Furthermore, although the involvement of PKA is not shown, the phosphorylation of proteasome subunits alters the status of proteasome assembly [23,24]. In the present study, we firstly showed that PKA activation enhanced the proteasome assembly, which contributed to the increase in proteasome activity. These findings suggest that altering proteasome subunit configuration through directed assembly by PKA may lead to the increase in proteasome activity, although we cannot exclude the possibility that PKA-mediated phosphorylation of proteasome subunits directly activates proteasome. Further investigation will be needed to clarify what subunit of proteasome is phosphorylated by PKA and the direct association between phosphorylation and assembly.

4.2. PKA stimulation enhances assembly and activity in in vivo canine hearts without affecting the total protein levels of proteasome subunits

Since proteasome activity is regulated by the multiple factors such as intracellular ATP levels and post-translational modification of proteasome [9,10], the in vitro findings of proteasome regulation are not always applied in the vivo model. Thus, to clarify whether the in vitro findings were also valid in vivo, we examined whether PKA stimulation could modulate proteasome assembly and activity in canine hearts. We employed two maneuvers to activate PKA in vivo, which were isoproterenol and forskolin as an exogenous stimulant of PKA [18,25] and IP as an endogenous stimulant [15]. We confirmed that both exogenous and endogenous stimulation of PKA enhanced 26S proteasome activity at 30 min after administration without changing the total protein levels of proteasome subunits in in vivo canine hearts. To our knowledge, the present study is the first to show the intervention to increase proteasome activity in vivo, suggesting that the pathophysiological conditions due to proteasome dysfunction in hearts could be treated.

We have found both 20S (α7 and β5) and 19S (Rpt5) subunit proteins in fractions where proteasome activity was detected, indicating that 26S proteasome was indeed eluted in these fractions. We confirmed that exogenous and endogenous PKA stimulation increased the protein levels of proteasome subunits in these fractions without changing total amount of proteasome subunits. These findings suggest that PKA stimulation enhanced 26S proteasome assembly as well as activity in in vivo canine hearts.

4.3. Time-course changes in proteasome activity during ischemia/reperfusion period with and without IP

To examine the time-course changes in proteasome activity during ischemia/reperfusion period, we performed myocardial biopsy at 4 time-points during ischemia/reperfusion period: at the control, just before ischemia (pre-ischemia), at the end of 90 min ischemia (post-ischemia) and 6 h of reperfusion (post-reperfusion). Previous study indicated that proteasome activity was decreased after ischemia/reperfusion [8]. Consistent with the previous report, the proteasome activity at the post-ischemia was significantly decreased compared with that at the control or pre-ischemia in groups without IP. Meanwhile, the proteasome activity at the post-ischemia was significantly lower than that at the pre-ischemia (=just after IP), however, it did not differ from the control in groups with IP (Fig. 7). These findings suggest that stimuli during ischemic period decreased myocardial proteasome activity and that proteasome activation by IP during ischemic period may play an important role in the protein turnover and cellular functions in ischemia/reperfusion hearts. Myocardial proteasome activity at the end of reperfusion did not differ from that at the end of ischemia in groups with and without IP, suggesting that stimuli during reperfusion did not significantly affect proteasome activity. Unfortunately, due to the small volume of biopsy samples, we could not check the time-course changes in the status of proteasome assembly.

4.4. IP blunts the accumulation of ubiquitinated proteins in ischemia/reperfusion myocardium

Recently, the ubiquitination of proteins is important post-translational processes that modify the functions of many proteins. We and others have reported that the accumulation of ubiquitinated protein in hearts was associated with the progression of cardiac dysfunction due to apoptosis [7,26]. In addition, the injured myocardium by ischemia/reperfusion is concomitant with a reduced proteasome activity [8]. Consistent with these previous reports, we found the decreased proteasome activity and the accumulation of ubiquitinated proteins in the ischemia/reperfusion myocardium. Interestingly, we found the less accumulation of ubiquitinated proteins in ischemia/reperfusion myocardium, which may be attributable to the 40% increase in proteasome activity by endogenous PKA stimulation. Since the accumulation of ubiquitinated proteins may predict recovery of postischemic cardiac function [21], the removal of damaged proteins due to proteasome activation by IP may contribute to improve postischemic cardiac function.

4.5. Proteasome inhibition did not alter infarct size in canine hearts with and without IP

Finally, we examined whether proteasome activation by IP contributed to its infarct-size limiting effects in the canine model. The infarct-size limiting effects of IP were not prevented by the intracoronary administration of epoxomicin, a proteasome inhibitor, at the dose that reduces proteasome activity by 43%. These findings suggest that proteasome activation by IP was not involved in the infarct-size limiting effects of IP in the acute phase. Future studies will be required about the pathophysiological role of proteasome activation in the chronic phase after myocardial infarction. Moreover, the intracoronary administration of epoxomicin itself could not reduce the infarct size in this model. This data was inconsistent with the previous ones that the inhibition of proteasome could reduce myocardial infarct size in rats and pigs [27,28]. The discrepancy between the previous and our studies might be due to the differences in animals used, experimental protocols and the drugs used. Further investigation will be needed to clarify whether reduced proteasome activity is beneficial or detrimental in the ischemia/reperfusion injury in the acute phase.

In conclusion, the present study demonstrated that PKA rapidly enhances proteasome activity and assembly in the in vivo heart. Modulation of proteasome activity and assembly might be a promising new therapeutic approach for cardiovascular diseases.

Acknowledgments

We thank Saori Ikezawa and Yoko Hamada for their technical assistance, and Kieko Segawa for the secretarial work. This work is supported by Grants-in-aid from the Ministry of Health, Labor, and Welfare-Japan and Grants-in-aid from the Ministry of Education, Culture, Sports, Science and Technology-Japan and Grants from the Japan Heart Foundation and Grants from the Japan Cardiovascular Research Foundation.

References

[1] Hershko A, Ciechanover A. The ubiquitin system. Annu Rev Biochem 1998;67:425–79.
[2] Hochstrasser M. Ubiquitin, proteasomes, and the regulation of intracellular protein degradation. Curr Opin Cell Biol 1995;7:215–23.
[3] Glickman MH, Ciechanover A. The ubiquitin–proteasome proteolytic pathway: destruction for the sake of construction. Physiol Rev 2002;82:373–428.
[4] Powell SR. The ubiquitin–proteasome system in cardiac physiology and pathology. Am J Physiol Heart Circ Physiol 2006;291:H1–H19.
[5] Voges D, Zwickl P, Baumeister W. The 26S proteasome: a molecular machine designed for controlled proteolysis. Annu Rev Biochem 1999;68:1015–68.
[6] DeMartino GN, Slaughter CA. The proteasome, a novel protease regulated by multiple mechanisms. J Biol Chem 1999;274:22123–6.
[7] Tsukamoto O, Minamino T, Okada K, Shintani Y, Takashima S, Kato H, et al. Depression of proteasome activities during the progression of cardiac dysfunction in pressure-overloaded heart of mice. Biochem Biophys Res Commun 2006;340:1125–33.
[8] Bulteau AL, Lundberg KC, Humphries KM, Sadek HA, Szweda PA, Friguet B, et al. Oxidative modification and inactivation of the proteasome during coronary occlusion/reperfusion. J Biol Chem 2001;276:30057–63.
[9] Zolk O, Schenke C, Sarikas A. The ubiquitin–proteasome system: focus on the heart. Cardiovasc Res 2006;70:410–21.
[10] Wang X, Robbins J. Heart failure and protein quality control. Circ Res 2006;99:1315–28.
[11] Zong C, Gomes AV, Drews O, Li X, Young GW, Berhane B, et al. Regulation of murine cardiac 20S proteasomes: role of associating partners. Circ Res 2006;99:372–80.
[12] Zhang F, Hu Y, Huang P, Toleman CA, Paterson AJ, Kudlow JE. Proteasome function is regulated by cyclic AMP-dependent protein kinase through phosphorylation of Rpt6. J Biol Chem 2007;282:22460–71.
[13] Wang Z, Aris VM, Ogburn KD, Soteropoulos P, Figueiredo-Pereira ME. Prostaglandin J2 alters pro-survival and pro-death gene expression patterns and 26 S proteasome assembly in human neuroblastoma cells. J Biol Chem 2006;281:21377–86.
[14] Fujita M, Asanuma H, Hirata A, Wakeno M, Takahama H, Sasaki H, et al. Prolonged transient acidosis during early reperfusion contributes to the cardioprotective effects of postconditioning. Am J Physiol Heart Circ Physiol 2007;292:H2004–8.
[15] Sanada S, Asanuma H, Tsukamoto O, Minamino T, Node K, Takashima S, et al. Protein kinase A as another mediator of ischemic preconditioning independent of protein kinase C. Circulation 2004;110:51–7.
[16] Sanada S, Kitakaze M, Papst PJ, Asanuma H, Node K, Takashima S, et al. Cardioprotective effect afforded by transient exposure to phosphodiesterase III inhibitors: the role of protein kinase A and p38 mitogen-activated protein kinase. Circulation 2001;104:705–10.
[17] Minamino T, Kitakaze M, Asanuma H, Tomiyama Y, Shiraga M, Sato H, et al. Endogenous adenosine inhibits P-selectin-dependent formation of coronary thromboemboli during hypoperfusion in dogs. J Clin Invest 1998;101:1643–1653.
[18] Kitakaze M, Hori M, Sato H, Takashima S, Inoue M, Kitabatake A, et al. Endogenous adenosine inhibits platelet aggregation during myocardial ischemia in dogs. Circ Res 1991;69:1402–8.
[19] Ogita H, Node K, Asanuma H, Sanada S, Liao Y, Takashima S, et al. Amelioration of ischemia- and reperfusion-induced myocardial injury by the selective estrogen receptor modulator, raloxifene, in the canine heart. J Am Coll Cardiol 2002;40:998–1005.
[20] Gomes AV, Zong C, Edmondson RD, Li X, Stefani E, Zhang J, et al. Mapping the murine cardiac 26S proteasome complexes. Circ Res 2006;99:362–71.
[21] Minamino T, Gaussin V, DeMayo FJ, Schneider MD. Inducible gene targeting in postnatal myocardium by cardiac-specific expression of a hormone-activated Cre fusion protein. Circ Res 2001;88:587–92.
[22] Powell SR, Wang P, Katzeff H, Shringarpure R, Teoh C, Khaliulin I, et al. Oxidized and ubiquitinated proteins may predict recovery of postischemic cardiac function: essential role of the proteasome. Antioxid Redox Signal 2005;7:538–546.
[23] Satoh K, Sasajima H, Nyoumura KI, Yokosawa H, Sawada H. Assembly of the 26S proteasome is regulated by phosphorylation of the p45/Rpt6 ATPase subunit. Biochemistry 2001;40:314–9.
[24] Bose S, Stratford FL, Broadfoot KI, Mason GG, Rivett AJ. Phosphorylation of 20S proteasome alpha subunit C8 (alpha7) stabilizes the 26S proteasome and plays a role in the regulation of proteasome complexes by gamma-interferon. Biochem J 2004;378:177–84.
[25] Mutafova-Yambolieva VN, Smyth L, Bobalova J. Involvement of cyclic AMP-mediated pathway in neural release of noradrenaline in canine isolated mesenteric artery and vein. Cardiovasc Res 2003;57:217–24.
[26] Powell SR, Gurzenda EM, Teichberg S, Mantell LL, Maulik D. Association of increased ubiquitinated proteins with cardiac apoptosis. Antioxid Redox Signal 2000;2:103–12.
[27] Pye J, Ardeshirpour F, McCain A, Bellinger DA, Merricks E, Adams J, et al. Proteasome inhibition ablates activation of NF-kappa B in myocardial reperfusion and reduces reperfusion injury. Am J Physiol Heart Circ Physiol 2003;284:H919–26.
[28] Campbell B, Adams J, Shin YK, Lefer AM. Cardioprotective effects of a novel proteasome inhibitor following ischemia and reperfusion in the isolated perfused rat heart. J Mol Cell Cardiol 1999;31:467–76.

Available online at www.sciencedirect.com
ScienceDirect
Biochemical and Biophysical Research Communications 365 (2008) 541–547
BBRC
www.elsevier.com/locate/ybbrc

Identification of a novel substrate for TNFα-induced kinase NUAK2

Hiroyuki Yamamoto [a], Seiji Takashima [b,c,*], Yasunori Shintani [b], Satoru Yamazaki [d], Osamu Seguchi [d], Atsushi Nakano [d], Shuichiro Higo [b], Hisakazu Kato [b], Yulin Liao [d], Yoshihiro Asano [b], Tetsuo Minamino [b], Yasushi Matsumura [a], Hiroshi Takeda [a], Masafumi Kitakaze [d]

[a] *Department of Medical Information Science, Osaka University Graduate School of Medicine, Suita, Osaka 565-0871, Japan*
[b] *Department of Cardiovascular Medicine, Osaka University Graduate School of Medicine, 2-2 Yamadaoka, Suita, Osaka 565-0871, Japan*
[c] *Health Care Center, Osaka University Graduate School of Medicine, Suita, Osaka 565-0871, Japan*
[d] *Department of Cardiovascular Medicine, National Cardiovascular Center, Suita, Osaka 565-8565, Japan*

Received 2 November 2007
Available online 20 November 2007

Abstract

TNFα has multiple important cellular functions both in normal cells and in tumor cells. To explore the role of TNFα, we identified NUAK family, SNF1-like kinase 2 (NUAK2), as a TNFα-induced kinase by gene chip analysis. NUAK2 is known to be induced by various cellular stresses and involved in cell mortality, however, its substrate has never been identified. We developed original protocol of de novo screening for kinase substrates using an in vitro kinase assay and high performance liquid chromatography (HPLC). Using this procedure, we identified myosin phosphatase target subunit 1 (MYPT1) as a specific substrate for NUAK2. MYPT1 was phosphorylated at another site(s) by NUAK2, other than known Rho-kinase phosphorylation sites (Thr696 or Thr853) responsible for inhibition of myosin phosphatase activity. These data suggests different phosphorylation and regulation of MYPT1 activity by NUAK2.

Keywords: NUAK family, SNF1-like kinase 2 (NUAK2); Myosin phosphatase target subunit 1 (MYPT1); TNFα; Myosin phosphatase; In vitro kinase assay

Tumor necrosis factor (TNFα) has multiple cellular functions both in normal cells and in tumor cells. TNFα not only induces apoptotic cell death but also enhances various gene expressions mediated by NFκB family transcriptional factors. Endothelial cells express TNFα receptors, and its NFκB-mediated signals induce various chemokine related molecules and cell adhesion molecules. These molecules enhance attachment of mononuclear cells and help these cells to enter into inflammatory tissues through endothelial cell barrier. TNFα also induces chemotactic molecules of endothelial cell, indicating that cell mobility induced by TNFα signal is mediated by as yet unidentified molecular mechanisms [1].

In the current study, we demonstrated that NUAK family, SNF1-like kinase 2 (NUAK2) was identified as a TNFα-induced kinase in endothelial cells by gene chip analysis. NUAK2 was originally identified in a PCR-based screen designed to identify a novel protein kinase [2]. Subsequent studies indicated that NUAK2 was induced by various cellular stresses such as ER stress, elevation of cellular AMP, hyperosmotic stress, and ultraviolet [3]. High expression of NUAK2 was also confirmed in various tumor cell lines [4], and overexpression of NUAK2 was reported to render tumor cell resistance under apoptotic stimuli. Such inductions and expressional mechanisms of NUAK2 have

* Corresponding author. Address: Department of Cardiovascular Medicine, Osaka University Graduate School of Medicine, 2-2 Yamadaoka, Suita, Osaka 565-0871, Japan. Fax: +81 6 8679 3473.
E-mail address: takasima@medone.med.osaka-u.ac.jp (S. Takashima).

0006-291X/$ - see front matter © 2007 Elsevier Inc. All rights reserved.
doi:10.1016/j.bbrc.2007.11.013

been well reported, however its substrate has never been identified.

Diverse effects of kinases in various tissues depend on specific substrates. To reveal the function of kinase it is essential to purify its substrate. Here, we identified myosin phosphatase target subunit 1 (MYPT1) as a specific substrate for NUAK2 using unique purification procedure. This method was designed to purify target substrates by combination of an in vitro kinase assay and high performance liquid chromatography (HPLC). NUAK2 phosphorylated MYPT1 at a distinct site(s) other than known Rho-kinase (ROCK) phosphorylation sites (Thr696 or Thr853) responsible for inhibition of myosin phosphatase activity, suggesting different phosphorylation and regulation of MYPT1 activity by NUAK2.

Materials and methods

Cell lines and reagents. Human umbilical vein endothelial cells (HUVECs) and human aortic smooth muscle cells (AoSMCs) were obtained from Clonetics. They were cultured in endothelial and smooth muscle cell medium (Clonetics) and used up to passage 5. HEK293T cells and HeLa cells were cultured in DMEM with 10% FBS. The following antibodies were purchased: anti-Flag (M2Ab; Sigma), anti-V5 (Invitrogen), anti-Myc (Invitrogen), anti-Tubulin (Cell Signaling), anti-NUAK2 (Abgent), anti-MYPT1 (BD Biosciences), anti-phospho-MYPT1 (Thr696) (Upstate Biotechnology), and anti-phospho-MYPT1 (Thr853) (CycLex). The following reagents were purchased: Trypsin (Promega), Lipofectamine 2000 (Invitrogen), Flag peptide (Sigma), and human recombinant TNFα (R&D Systems, Inc.).

cDNA microarray analysis. To determine the effect of TNFα on gene expression profile, we treated cultured HUVECs without or with TNFα (20 ng/ml) for 2 h, and then performed cDNA microarray studies. Total RNA was prepared from HUVECs using RNA-Bee-RNA Isolation Reagent (Tel-Test Inc.) according to the manufacturer's instructions. Microarray hybridization was performed in triplicate using Affymetrix Human Genome 133A gene chips (HG-U133A). After synthesizing double-stranded cDNA from the total RNA, an in vitro transcription reaction was done to produce biotin-labeled cRNA from cDNA, and the cRNA was fragmented before hybridization. Hybridization, probe washing, staining and probe array scanning were performed following the protocols provided by Affymetrix. Data were analyzed using Genespring 6 software [5]. Normalization was done by a combination of three steps: rewriting negative values as 0.01, normalizing to the 50th percentile per chip and normalizing to the median per gene. We filtered data using a combination of parameters such as signal confidence ('present' flag), fold change (>3), minimum acceptable signal intensity (average difference ≥50 in at least one of the two groups). Indicated gene accession numbers were derived from the GenBank database.

Northern blot analysis. Northern blot analysis was performed as previously described [6]. Briefly, total RNA was isolated and electrophoresed on 1% agarose gel containing 2.2 M formaldehyde, and transferred onto nylon membranes (Bio-Rad). The membranes were hybridized with ^{32}P-labeled fragments of human cDNA corresponding to nucleotides 1–1887 of NUAK2 cDNA. A BAS photoimaging system (Fuji) was used for detection.

Quantitative RT–PCR. Total RNA was extracted using RNA-Bee-RNA Isolation Reagent (Tel-Test Inc.). Then, 1 μg of total RNA was reverse-transcribed using Omniscript RT (Qiagen) according to the manufacturer's protocol. Quantitative RT-PCR was performed with TaqMan technology using the ABI Prism 7000 detection system (Applied Biosystems) according to the manufacturer's instructions. RT-PCR conditions were 2 min at 50 °C, 10 min at 95 °C, and 40 cycles of 15 s at 95 °C and 1 min at 60°C. Data were normalized to 18S ribosomal RNA or GAPDH level. Each sample was analyzed in duplicate and the experiments were replicated three times. For 18S ribosomal RNA, GAPDH and NUAK2, primers and probes were obtained using TaqMan Assays-on-Demand gene expression products (Applied Biosystems).

Cloning, plasmid construction, and mutagenesis. In this experiment, all construction was performed using the Gateway system (Invitrogen) according to the manufacturer's instructions. Human NUAK2 cDNA was isolated from HUVECs cDNA using the following sense and antisense primers: sense 5′ caccatggagtcgctggtttttcg and antisense 5′ tcaggtgagctttgagcagaccc. With PCR primer designed to include stop codon of NUAK2, the amplified fragment was inserted into pENTR/D-TOPO (Invitrogen), named pENTR/NUAK2. To generate N-terminal Flag-tagged NUAK2 (Flag-NUAK2), Flag epitope (DYKDDDDK) was introduced into just before the N terminus of NUAK2 by PCR-based mutagenesis using pENTR/NUAK2 as a template. The NUAK2 constructs were recombined to mammalian expression vector, pcDNA3.1 vector (Invitrogen). We also generated N-terminal Myc-tagged NUAK2 (Myc-NUAK2) using the same protocol. cDNA encoding human MYPT1 was generated by RT-PCR with RNA from HUVECs. The mammalian expression vectors for MYPT1 were constructed using pENTR/D-TOPO (pENTR-MYPT1). To identify the binding site on MYPT1 for NUAK2, pENTR-Flag-MYPT1 D1 lacking aa 11–286, pENTR-Flag-MYPT1 D2 lacking aa 287–514, pENTR-Flag-MYPT1 D3 lacking aa 515–799 or pENTR-Flag-MYPT1 D4 lacking aa 800–1020 were generated by PCR using pENTR-MYPT1 as a template. An *Escherichia coli* expression vector for GST-MYPT1 was constructed using the expression vector, pGEX5X-1 (Pharmacia) and cDNA encoding MYPT1 protein. Expression plasmids for mutated NUAK2 and mutated MYPT1 were generated using the QuickChange site-directed mutagenesis kit (Stratagene) following the manufacturer's instructions. All constructs were verified by sequencing.

Co-immunoprecipitation assay. HEK293T cells were transfected with 5 μg cDNA/60 mm dish using Lipofectamine 2000. Two days after transfection, cells were lysed in lysis buffer (1% Nonidet P-40, 0.15 M NaCl, 20 mM Tris, pH 7.2, and 2 mM EDTA including protease inhibitor cocktail (Nacalai)). We then incubated with anti-V5, anti-Myc or anti-Flag agarose for 1 h at 4 °C. After extensive washing, immunoprecipitated samples were subjected to SDS–PAGE and immunoblotting was performed as described previously [7].

In vitro kinase assay. The following recombinant proteins were purchased: human NUAK2 (Cell Signaling), and ROCK-II, human active (Upstate Biotechnology). Bacterially purified glutathione S-transferase (GST) fusing proteins were used as substrates. Recombinant proteins were equilibrated in kinase buffer [0.15 M NaCl, 20 mM MOPS (pH 7.0), 10 μM $MgCl_2$, 10% glycerol, and 1 mM DTT], and then incubated with 10 μCi of [γ-^{32}P] ATP (Amersham) and substrates at 30 °C for 60 min. Each sample was boiled in SDS sample buffer for 3 min, and eluted proteins were analyzed by SDS–PAGE. The gel was dried and autoradiographed. ROCK-II, human active (0.317 pmol) and NUAK2 (1.33 pmol) were used in this assay.

Identification of a NUAK2-binding protein (p130). We used HEK293T cells expressing pcDNA3.1-Flag-tagged-NUAK2, lysed them with 1 ml of lysis buffer and immunoprecipitated them with anti-Flag antibody followed by elution with Flag peptide (100 μg/ml). An in vitro kinase assay was performed with the eluate in the presence of [γ-^{32}P] ATP followed by SDS–PAGE, and the radioactivity was detected by a BAS imaging analyzer (Fuji). The FLAG peptide eluate was injected onto a phenyl-reverse phase—HPLC column (4.6 × 250 mm, Nacalai) equilibrated with 0.1% trifluoroacetic acid and 5% acetonitrile. Fractions were eluted with a linear gradient of 35–45% acetonitrile at a flow rate of 1 ml/min. Each fraction was lyophilized and separated by SDS–PAGE. Radioactivity was detected by BAS imaging system.

Data analysis. Statistical significance was assessed with ANOVA using the Fisher's post hoc test. A value of $p < 0.05$ was considered to be statistically significant.

Table 1
Expression levels and fold change of the upregulated genes by TNFα in HUVECs (top 20)

Gene name	Accession No.	Control group	TNFα group	Fold change (TNFα/Control)
CCL20	NM_004591.1	0.04	7.33	168.20
E-selectin	NM_000450.1	0.08	5.11	70.63
IL-8	NM_000584.1	0.16	8.16	50.35
Coagulation factor III	NM_001993.2	0.29	7.17	24.96
TNFAIP3	NM_006290.1	0.21	4.08	19.05
VCAM1	NM_001078.1	0.16	3.03	18.95
CXCL3	NM_002090.1	0.27	5.07	18.46
CXCL2	NM_002089	0.34	4.99	14.68
TNFAIP2	NM_006291.1	0.26	3.55	13.52
CXCL1	NM_001511.1	0.32	3.70	11.70
CXCR7	NM_020311	0.37	4.02	10.77
ICAM1	NM_000201.1	0.23	2.36	10.34
TNFAIP8	NM_014350.1	0.50	5.01	9.95
Ephrin-A1	NM_004428.1	0.26	2.24	8.63
CD69 antigen	NM_001781.1	0.53	3.93	7.43
CX3CL1	NM_002996	0.36	2.46	6.75
RND1	NM_014470	0.32	2.04	6.37
PMAIP1	NM_021127.1	0.73	4.58	6.26
NUAK2	NM_030952.1	0.31	1.91	6.24
CCL2	NM_002982	0.42	2.47	5.87

HUVECs were stimulated with TNFα (20 ng/ml) (TNFα group) or medium only (Control) for 2 h. Every time, a pair of TNFα and Control was used for cDNA microarray examination, which was repeated for three times in different date. Data are mean for the three times. Only the genes that were upregulated by TNFα for more than 3-folds every times were included in this table. The expression levels were normalized intensity (linear scale).

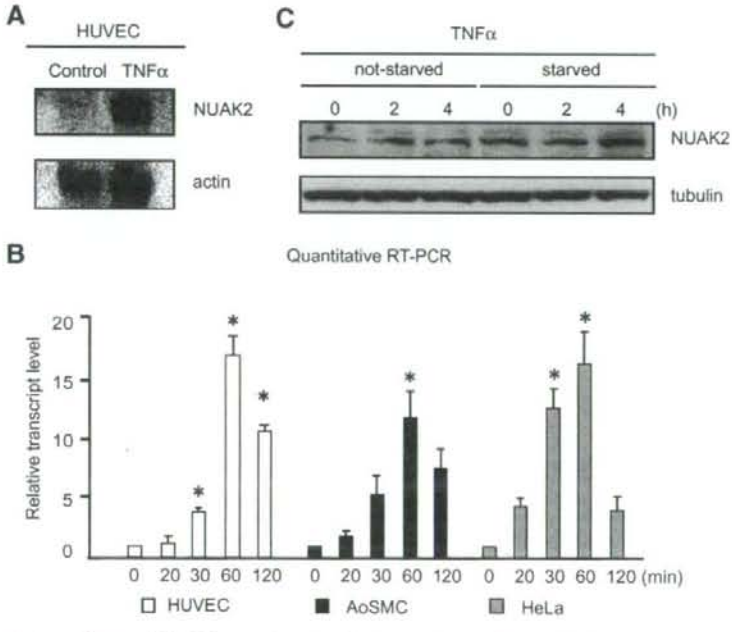

Fig. 1. TNFα induces upregulation of human NUAK2 expression. (A) Northern blot analysis. HUVECs were treated with TNFα (20 ng/ml) for 2 h or control. Total RNA was harvested, electrophoresed, and blotted to the nitrocellulose membrane. The membrane was probed with cDNA for human NUAK2. Beta actin was used as an internal control for mRNA loading. (B) Time course of NUAK2 mRNA levels. Various cell lines were treated with TNFα (20 ng/ml) for the indicated times. Each sample was analyzed in duplicate and experiments were performed in triplicate. (C) HeLa cells were either not starved or starved for 18 h in DMEM containing 0.5% serum. Starved and unstarved cells were then treated with TNFα (20 ng/ml) for indicated times. Cells were lysed and immunoblotting was performed with the indicated antibodies. For panels B, error bars represent SEM. $^{*}P < 0.05$ versus baseline.

Results

TNFα induced NUAK2 mRNA and protein expressions

To identify the specific expression targets of TNFα, the profiles of mRNA expression extracted from HUVECs were analyzed. Triplicate assay of gene chip revealed that 57 genes were enhanced their expressions 2 h after TNFα treatment. Most of these genes increased more than 3-folds are chemokines and their related molecules such as their receptors, adhesion molecules, and transcription factors (Table 1). Among them, one kinase, NUAK2, was greatly enhanced its expression by TNFα. No other kinases were enhanced its expression more than 3-folds, suggesting that NUAK2 is only a strongly inducible kinase by TNFα signaling in endothelial cells. This result was confirmed by Northern blot analysis (Fig. 1A). Quantitative PCR revealed that an enhanced NUAK2 expression after TNFα treatment was seen not only in HUVECs but also in other cell lines in a time-dependent manner (Fig. 1B). Increasing protein level by TNFα was also confirmed by immunoblotting with anti-NUAK2 antibody (Fig. 1C).

NUAK2-associated kinase activity

Since the substrate for NUAK2 has not been identified, we screened a protein which bound to NUAK2 and was phosphorylated by NUAK2. We employed a kinase-dead construct of NUAK2 (Flag-KD-NUAK2) in which Lys81 was replaced with Arg as a control. HEK293T cells were transiently transfected with Flag-WT-NUAK2 or Flag-KD-NUAK2. Immunoprecipitation assay was performed with whole-cell extracts using anti-Flag antibody followed by elution with Flag peptide. An in vitro kinase assay was performed with the eluate in the presence of [γ-^{32}P] ATP. NUAK2 was autophosphorylated in vitro [4]. Besides NUAK2 radioactivity, a phosphorylated band at the size of 130 kDa (p130) was co-immunoprecipitated

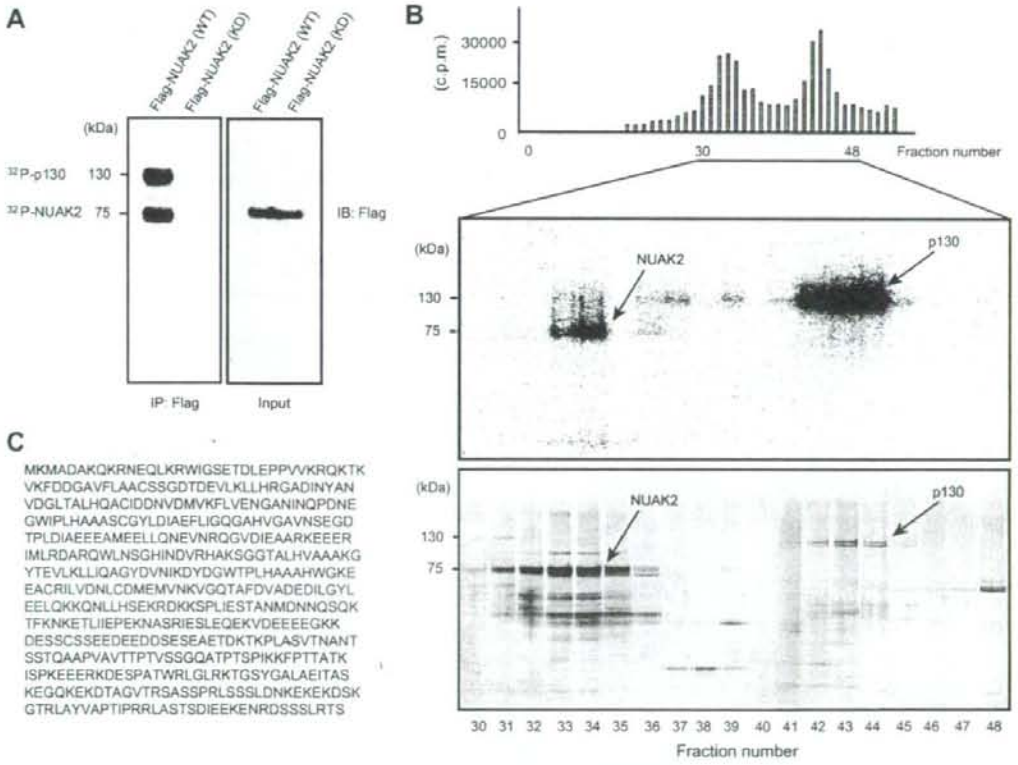

Fig. 2. Purification and identification of MYPT1. (A) HEK293T cells were transiently transfected with Flag-WT-NUAK2 or Flag-KD-NUAK2. Immunoprecipitation assay was performed with whole-cell extracts using anti-Flag antibody followed by elution with Flag peptide. An in vitro kinase assay was performed with the eluate in the presence of [γ-^{32}P] ATP (left panel). The lysates were immunoblotted with anti-Flag antibody (right panel). (B) The complex of radiolabeled NUAK2 and p130 was separated by a phenyl reverse-phase column and indicated fractions were quantified for phosphorylation of the complex (upper panel). These proteins in the indicated fractions were resolved by SDS–PAGE followed by autoradiography (middle panel). Large-scale purification of the protein complex was done using the same protocol without radioactive material. The purified products of the protein complex were resolved on SDS–PAGE and silver stained (lower panel). (C) Amino acid sequence of human MYPT1. The peptides derived from the purified protein (p130), which fitted with those of human MYPT1 as assessed by mass spectrometry, are shown in bold red. (For interpretation of the references to color in this figure legend, the reader is referred to the web version of this article.)

(Fig. 2A). In the control lane, neither NUAK2 nor p130 could be detected, suggesting that p130 was a NUAK2-binding substrate.

Purification of NUAK2 substrate

To characterize p130, we applied the Flag eluate to a reverse phase column. There were two radioactive peaks (fraction numbers 32–34, 42–44) detected in these fractions (Fig. 2B, upper panel) and each fraction was electrophoresed followed by autoradiography (Fig. 2B, middle panel). NUAK2 and p130 were well separated and matched to radioactive peak. To identify p130, we scaled up the purification procedure using HEK293T cells (4.0×10^7) expressing Flag-tagged NUAK2 without radioactive material. The purified products of the protein complex were resolved by SDS–PAGE and silver stained. Silver staining of these fractions detected NUAK2 and p130 (Fig. 2B, lower panel). We analyzed the peptides digested from the p130 band by mass spectrometry. P130 included fragments of the amino acid sequences of WIGSETDLEPPVVKR, QWLNSGHINDVR and LAYVAPTIPR that matched human myosin phosphatase targeting subunit 1 (MYPT1) (Fig. 2C).

MYPT1 is associated with NUAK2

To test whether MYPT1 is associated with NUAK2, HEK293T cells were transiently transfected with or without Myc-NUAK2. Protein extracts were subjected to immunoprecipitation with anti-Myc antibody, followed by immunoblotting with anti-MYPT1 antibody. We confirmed direct binding of endogenous MYPT1 to recombinant NUAK2 (Fig. 3A). Next, to identify the binding site on MYPT1 for NUAK2, we constructed several MYPT1 deletion mutants (Fig. 3B). Mutation analysis revealed that the NUAK2-binding domain corresponded to the C-terminal domain (amino acids 800–1020) of MYPT1 (Fig. 3C).

In vitro phosphorylation of MYPT1 by NUAK2

Recombinant human NUAK2 purified by baculovirus expression system efficiently phosphorylated *E. coli* recombinant MYPT1, suggesting that NUAK2 directly phosphorylates MYPT1 (Fig. 4A). Rho-kinase (ROCK) is

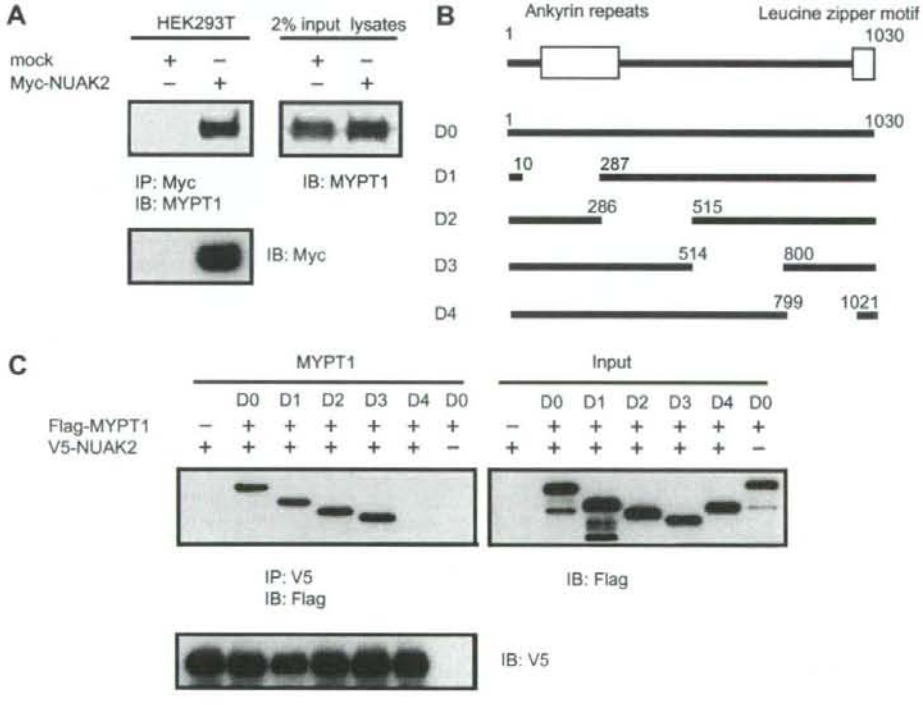

Fig. 3. NUAK2 interacts with MYPT1. (A) HEK293T cells were transiently transfected with mock or Myc-tagged NUAK2. Whole-cell extracts were subjected to immunoprecipitation assays using anti-Myc antibody followed by immunoblotting using anti-MYPT1 antibody. The same filter was reprobed with anti-Myc antibody. The same lysates were also analyzed by immunoblotting using anti-MYPT1 antibody. (B) Schematic model of the MYPT1 deletion mutants. The numbers are the amino acid number. (C) HEK293T cells were transiently transfected with V5-tagged NUAK2, Flag-tagged WT or various truncated MYPT1, alone, or together as indicated. Co-immunoprecipitation assays were performed with whole-cell extracts using anti-V5 antibody, followed by immunoblotting using anti-V5 or anti-Flag antibodies. The same lysates were also analyzed by immunoblotting using anti-Flag antibody.